Original Article

The value of a deep learning image reconstruction algorithm in whole-brain computed tomography perfusion in patients with acute ischemic stroke

Limin Lei[1#], Yuhan Zhou[1#], Xiaoxu Guo[1], Luotong Wang[2], Xitong Zhao[1], Hui Wang[1], Jinping Ma[1], Songwei Yue[1]

[1]Department of Radiology, The First Affiliated Hospital of Zhengzhou University, Zhengzhou, China; [2]GE HealthCare China, Beijing, China

Contributions: (I) Conception and design: L Lei, S Yue; (II) Administrative support: S Yue; (III) Provision of study materials or patients: Y Zhou, X Zhao; (IV) Collection and assembly of data: L Lei, H Wang, J Ma; (V) Data analysis and interpretation: L Lei, X Guo, L Wang; (VI) Manuscript writing: All authors; (VII) Final approval of manuscript: All authors.

[#]These authors contributed equally to this work.

Correspondence to: Songwei Yue, MD. Department of Radiology, the First Affiliated Hospital of Zhengzhou University, 1 Jianshe East Road, Zhengzhou 450052, China. Email: ysw197281@sina.com.

Background: Computed tomography perfusion (CTP) and computed tomography angiography (CTA) are valuable tools for diagnosing acute ischemic stroke (AIS). It is essential to obtain high-quality CTP and CTA images in short time. This study aimed to evaluate the image quality and diagnostic performance of brain CTP and CTA images generated from CTP reconstructed by a deep learning image reconstruction (DLIR) algorithm on patients with AIS.

Methods: The study prospectively enrolled 54 patients with suspected AIS undergoing non-contrast CT and CTP within 24 hours. CTP datasets were reconstructed with three levels of adaptive statistical iterative reconstruction-Veo algorithm [ASIR-V 0% with filtered back projection (FBP), ASIR-V 40%, and ASIR-V 80%] and three levels of DLIR, including low (DLIR-L), medium (DLIR-M), and high (DLIR-H). CTA images were generated using the CTP datasets at the peak arterial phase. Objective parameters including signal-to-noise ratio (SNR), contrast-to-noise ratio (CNR), and noise reduction rate. Subjective evaluation was assessed according to Abels scoring system. Perfusion parameters and detection accuracy for infarction core lesions were evaluated. The objective and subjective image quality of CTA images were also evaluated.

Results: All reconstructions produced similar CT values (P>0.05). With the increase of ASIR-V and DLIR reconstruction strength, image noise decreased, while SNR and CNR increased for CTP images, especially in white matter. DLIR-H, DLIR-M, and ASIR-V80% yielded higher subjective scores than did ASIR-V40% and FBP. DLIR-H provided the highest noise reduction rate and detection accuracy. No significant difference was found in conventional parameters, the volume of infarct core, or ischemic penumbra among the 6 groups (P>0.05). The objective evaluation of reconstructed CTA images was comparable in DLIR-H, DLIR-M, and ASIR-V80% (P>0.05). The subjective scores of the DLIR-H and DLIR-M images were higher than those of the other groups, especially ASIR-V40% and FBP (P<0.05).

Conclusions: Compared with FBP and ASIR-V40%, DLIR-H, DLIR-M, and ASIR-V80% improved the overall image quality of CTP and CTA images to varying degrees. Furthermore, DLIR-H and DLIR-M showed the best performance. DLIR-H is the best choice in diagnosing AIS with improved detection accuracy for cerebral infarction. Reconstructing CTA images using CTP datasets could reduce contrast agent and radiation dose.

Keywords: Deep learning image reconstruction algorithm (DLIR algorithm); computed tomography perfusion (CTP); reconstructed CT angiography; image quality; acute ischemic stroke (AIS)

Submitted Apr 20, 2023. Accepted for publication Sep 19, 2023. Published online Oct 31, 2023.
doi: 10.21037/qims-23-547
View this article at: https://dx.doi.org/10.21037/qims-23-547

Introduction

Ischemic stroke is the leading cause of permanent disability and death worldwide, accounting for more than 80% of all stroke incidents (1). In recent years, ischemic stroke has had a youth-oriented tendency. Many randomized controlled trials, including the DAWN (Diffusion-Weighted Imaging or Computed Tomography Perfusion Assessment with Clinical Mismatch in the Triage of Wake-Up and Late Presenting Strokes Undergoing Neurointervention with Trevo) (2) and DEFUSE-3 (Endovascular Therapy Following Imaging Evaluation for Ischemic Stroke 3) trials (3), have confirmed the importance of computed tomography perfusion (CTP) in diagnosing acute ischemic stroke (AIS). CTP can quickly and accurately identify the ischemic penumbra and infarct core with postprocessing software such as Rapid Processing of Perfusion and Diffusion (RAPID) (4,5), which benefits patients who undergo endovascular thrombectomy. Moreover, studies have shown that computed tomography angiography (CTA) images reconstructed using CTP datasets can replace conventional CTA to evaluate vasospasm (6) and are able to evaluate the collateral circulation of patients with AIS, especially the reconstruction of multiphase CTA (7).

Due to the need to control the radiation dose caused by continuous scanning in CTP examination, the main concern that limits the clinical application of CTP is its image quality (8-11). Previous studies have shown that reconstruction algorithms can significantly affect image quality (12-14). Reducing the acquisition dose by three-quarters will double the noise of filtered back projection (FBP) reconstructions, while the same amount of dose reduction will only lead to a 40% increase in noise in nonlinear iterative reconstruction (IR) algorithms (15). Although the IR algorithms can overcome the shortcomings of the high noise and artifacts of FBP in low-dose scanning, its further development has been limited by the "plastic-like" or "waxy" image appearance produced by repeated iterations in high-intensity reconstruction (12,16). The deep learning image reconstruction (DLIR) algorithm (TrueFidelity, GE HealthCare, Milwaukee, WI, USA) is a newly developed deep neural network (DNN)-based reconstruction algorithm, which is based on high-dose FBP images put through numerous complex training, validation, and testing sets. The output images can dramatically reduce noise, while retaining noise texture and anatomical and pathological details (17). Several phantom and clinical studies in thoracic and abdominal applications have reported the advantages of DLIR over IR in reducing image noise, improving image quality, and accurately detecting low-contrast lesions (18-22).

Thus, our study aimed to compare the image quality of CTP and reconstructed CTA images, perfusion parameters, and AIS diagnostic accuracy of DLIR, adaptive statistical iterative reconstruction-Veo (ASIR-V), and FBP reconstruction.

Methods

This study was approved by the Human Research Ethics Committee of the First Affiliated Hospital of Zhengzhou University (No. 2022-KY-0929-002) and was conducted in accordance with the Declaration of Helsinki (as revised in 2013). All enrolled patients signed written informed consent forms.

Study population

From March to August 2022, patients with suspected AIS in the emergency green channel of our hospital were prospectively collected. The inclusion criteria were the following: (I) patients who underwent non-contrast head CT (NCCT) and CTP within 24 hours of symptom onset, (II) no previous history of large area ischemic stroke, and (III) at least 1 follow-up NCCT or magnetic resonance imaging (MRI) scan performed within 1 week of onset to determine the presence of cerebral infarction. The exclusion criteria were the following: (I) head trauma, tumor, or hemorrhagic disease; (II) poor CTP image quality due to excessive motion or failed contrast bolus; (III) patients with iodine contrast agent hypersensitivity; (IV) patients who had been treated before CT examination; (V) massive cerebral edema or bleeding after treatment resulting in the inaccuracy of infarction on CT or MRI images during the review.

Image acquisition

All CT acquisitions were performed on the latest-generation

256-row detector CT scanner (Revolution APEX, GE HealthCare), with a detector coverage of 160 mm. The whole scanning protocol involved head NCCT and CTP. Head NCCT was performed with the following imaging parameters: axial acquisition from skull base to vertex, tube voltage of 120 kV, automatic tube current modulation (100–500 mAs), noise index (NI) 2.5 Hounsfield units (HU), rotation time 0.8 s, matrix 512×512, and 5-mm slice thickness reconstruction.

The CTP acquisition parameters were as follows: axial acquisition from skull base to vertex, 80 kV tube voltage, 150 mA tube current, intermittent scan with a 5-mm section thickness, and 1.0 s rotation time. Additionally, 50 mL (350 mg I/mL) of iodinated contrast medium (iohexol, GE HealthCare) was power-injected into the right antecubital vein at the rate of 5 mL/s and followed by a 50 mL saline flush at the same rate. Scanning began with a 5-s delay after the contrast agent injection, with 12 passes performed at 2-s intervals and then 8 passes performed at 3-s intervals; the total scanning time was 48 s.

The system automatically recorded the volume CT dose index [CTDIvol; measured in milligray (mGy)] and dose length product (DLP; measure as mGy·cm). The effective radiation dose (ED) was the product of radiation weight factor K and DLP, as follows: ED = DLP × K. For brain examination, K=0.0023 mSv/(mGy·cm).

Image reconstruction

The CTP raw data were reconstructed using the following six reconstruction algorithms: ASIR-V with a 0% strength level (FBP), ASIR-V with strength level of 40% and 80% (ASIR-V40% and ASIR-V80%), and DLIR with three levels, including low DLIR (DLIR-L), medium DLIR (DLIR-M), and high DLIR (DLIR-H). The ASIR-V50% was commonly used as the standard IR reconstruction algorithm for the comparison between images reconstructed with IR and the DLIR algorithm. However, we wanted to conduct a comprehensive study, so, with reference to the study by Jiang *et al.* (20), we selected ASIR-V40% and ASIR-V80% for IR image reconstruction. The slice thickness and interval in reconstruction were both 5 mm, as is the case in routine clinical practice. In addition, CTA images with a slice thickness of 0.625 mm were reconstructed using the CTP datasets in the peak arterial phase with the above 6 algorithms.

Image quality evaluation of CTP

Objective image quality evaluation of CTP

All CTP data were transferred to an Advantage Workstation 4.7 (GE HealthCare), and CT Perfusion 4D software based on the deconvolution algorithm was used for image postprocessing. On the Average CTP map, the regions of interest (ROIs) with a diameter of 10 mm were manually drawn in the gray matter (GM) and white matter (WM) of the frontal, temporal, and parietal lobes on the contralateral side separately by a radiologist with 10 years of work experience, with blood vessels and cerebral sulci being avoided as much as possible (21,23,24). Finally, the average attenuation (in HU) and standard deviation (SD) of the corresponding peak arterial phase of the image were evaluated (*Figure 1A-1F*). All the ROIs were continuously sketched and measured three times at the same location ensured by ROIs copied among all six reconstructed groups, and the average values were finally compared. We defined the mean CT values (HU) of GM or WM at the frontal, temporal, and parietal lobes on the contralateral side as CT attenuation of GM or WM. The image noise of GM or WM was defined as the mean values of three regions.

Subsequently, the signal-to-noise ratio (SNR), contrast-to-noise ratio (CNR), and noise reduction rate of different reconstructions were calculated as follows (8):

$$SNR_{GM/WM} = \frac{\sum\left(CT_{frontal}+CT_{temporal}+CT_{parietal}\right)}{\sum\left(SD_{frontal}+\mathrm{SD}_{temporal}+SD_{parietal}\right)} \quad [1]$$

$$CNR = \frac{Mean\left(CT_{GM}\right)-Mean\left(CT_{WM}\right)}{\sqrt{Mean\left(SD_{GM}\right)^2-Mean\left(SD_{WM}\right)^2}} \quad [2]$$

$$Noise\ reduction\ rate_{GM} = \frac{Mean\left(SD_{FBP_{GM}}\right)-Mean\left(SD_{ASIR\text{-}V/DLIR_{GM}}\right)}{Mean\left(SD_{FBP_{GM}}\right)}\times 100\% \quad [3]$$

$$Noise\ reduction\ rate_{WM} = \frac{Mean\left(SD_{FBP_{WM}}\right)-Mean\left(SD_{ASIR\text{-}V/DLIR_{WM}}\right)}{Mean\left(SD_{FBP_{WM}}\right)}\times 100\% \quad [4]$$

In Eqs. [3,4], ASIR-V/DLIR indicated ASIR-40%, ASIR-V80%, DLIR-L, DLIR-M, or DLIR-H.

The parametric maps, including cerebral blood flow (CBF), cerebral blood volume (CBV), time to maximum (Tmax), mean transit time (MTT), and time to peak (TTP) were automatically generated, and these parameters were calculated at the same site the CT values were measured across all 6 reconstructed groups.

Subjective image quality evaluation of CTP

Subjective evaluation was conducted independently by

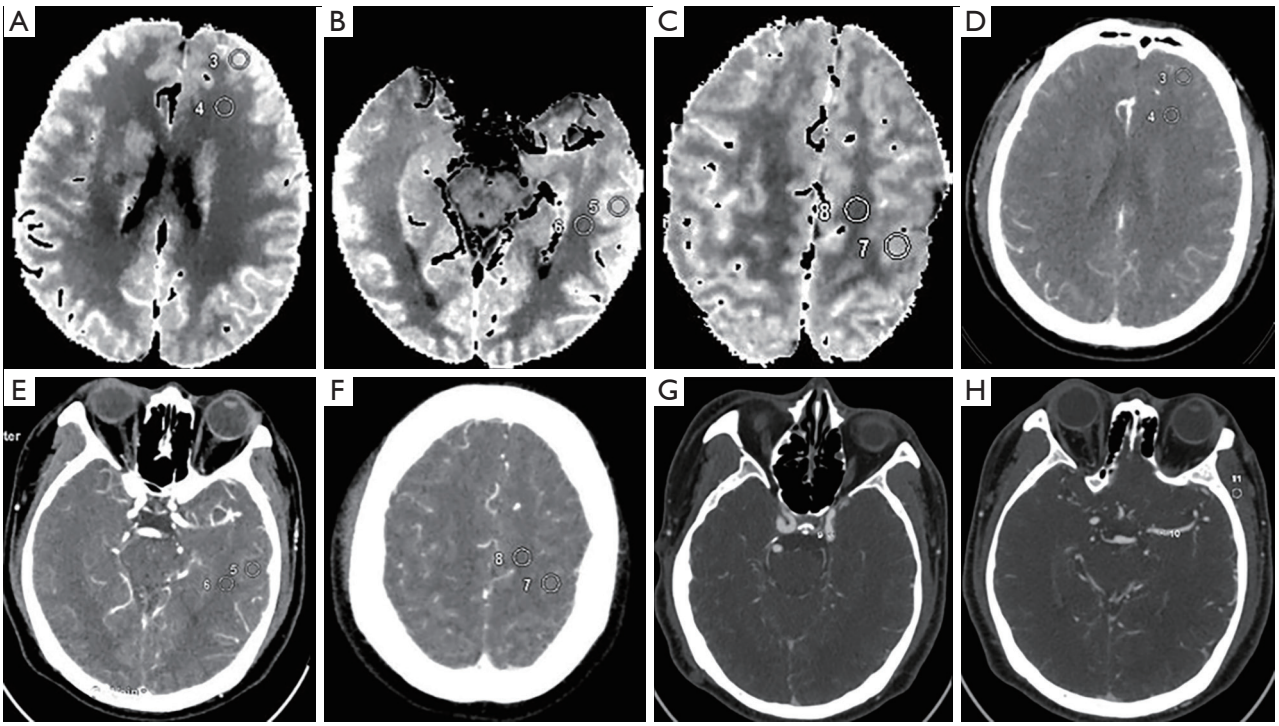

Figure 1 ROI positions in the evaluation of the CTP image and reconstructed CTA image. ROIs were sketched on the contralateral side on the average map (A-C), and CT value and SD value were measured on the CTP arterial peak phase (D-F). (A,D) GM (ROI3) and WM (ROI4) of the frontal lobe. (B,E) GM (ROI5) and WM (ROI6) of the temporal lobe. (C,F) GM (ROI7) and WM (ROI8) of the parietal lobe. (G,H) ROIs were sketched at the ICA siphon (ROI9), MCA-M1 (ROI10), and temporalis (ROI11) on the contralateral side of axial images of the CTP arterial peak phase. ROI, region of interest; CTP, computed tomography perfusion; CTA, computed tomography angiography; CT, computed tomography; SD, standard deviation; GM, gray matter; WM, white matter; ICA siphon, siphon of the internal carotid artery; MCA-M1, M1 segment of the middle cerebral artery.

two radiologists with 10 years of diagnostic experience. These two radiologists were blinded to the reconstruction settings and the results of the objective analysis. CT images from six reconstruction groups were randomly reviewed, and the radiologists evaluated the images using a 3-point scoring system (0= poor, 1= moderate, 2= good) on each of the following 4 categories (the same scoring method was used for Tmax as for MTT and TTP) as described in a previous CTP study (25): (I) GM-WM differentiation of CBF and CBV maps and grading of the MTT and TTP maps, (II) differentiation of ischemic and normal tissue, (III) homogeneity (contrast, contours, coherency/dissemination of the ischemic lesion), and (IV) compensation of artifacts. The scores of the four categories were added, resulting in a maximum score of 8. An image with >6 points was considered high quality and of high diagnostic value, an image with >3 points and ≤6 points was considered medium quality but still diagnostic, while an image with ≤3 points was considered poor quality and insufficient for diagnosis.

Diagnostic parameter assessment of CTP

Based on whether there was cerebral infarction on NCCT or MRI images reexamined within 1 week after onset, we evaluated the detection accuracy of lesions of the six reconstruction groups. In this procedure, the images were displayed randomly, and the radiologist took a 5-hour break after evaluating five sets of images (each set referred to 1 of the reconstructed images of a patient). The detection accuracy for lesions was calculated as follows:

$$Detection\ accuracy=\frac{Number\ of\ lesions\ detected\ by\ radiologists}{Total\ lesions}\times 100\% \quad [5]$$

On the tissue classification area of the CT Perfusion 4D software package, the volume of cerebral infarction and tissue at risk of all the six groups of images of patients with

AIS were evaluated automatically. Additionally, we imported all six groups of images into the automated, commercially available software platform RAPID (ISchemiaView Inc., Menlo Park, CA, USA). Within the CT Perfusion 4D software, the ischemic core was defined as a region with a reduction in the relative CBF <10% of that in the contralateral normal tissue, and a tissue at risk was defined as regions of Tmax >7 s (26). Within the RAPID software, the rCBF threshold was set to rCBF <30%, and the Tmax threshold was set to 6 s. The ischemic penumbral (mismatch volume) was calculated using the volume of tissue at risk minus the ischemic core volume (27).

Image quality evaluation of the reconstructed CTA from the CTP datasets

Objective image quality evaluation of the reconstructed CTA

Six groups of reconstructed intracranial CTA images were evaluated. The ROIs were delineated in the siphon of the internal carotid artery (ICA), M1 segment of the middle cerebral artery (MCA-M1), and the temporalis on the contralateral side of the axial images, and corresponding CT and SD values were measured. The ROI of the vascular region was greater than one-half of the lumen area to avoid areas affected by plaques or artifacts. The ROI of temporalis was not less than 10 cm^2 (*Figure 1G,1H*). All ROIs were sketched and measured three times at three consecutive image levels to calculate their average values, and the ROI of the six reconstruction groups of the same patient was placed in the same position via copying and pasting. The temporalis was used as a background because it provides homogeneous attenuation, and fat deposits were avoided. The SNR and CNR of the six groups of CTA images were calculated and compared. The calculation formulae were as follows:

$$SNR_{vessel/temporalis} = \frac{Mean\left(CT_{vessel/temporalis}\right)}{Mean\left(SD_{vessel/temporalis}\right)} \quad [6]$$

$$CNR_{vessel} = \frac{Mean\left(CT_{vessel}\right) - Mean\left(CT_{temporalis}\right)}{\sqrt{Mean\left(SD_{vessel}\right)^2 + Mean\left(SD_{temporalis}\right)^2}} \quad [7]$$

The SNR and CNR for the vessel of ICA siphon and MCA-M1 were calculated.

Subjective image quality evaluation of the reconstructed CTA

Two experienced radiologists evaluated the CTA images independently and reached a consensus through discussion when the results were inconsistent. The evaluation mainly included the following four aspects: (I) image noise, divided into four levels (level 1, image noise is too high to be diagnostic; level 2, image noise is high but still be diagnostic; level 3, image noise is moderate, diagnostic; level 4, little image noise, diagnostic); (II) edge sharpness of the vascular lumen, divided into four levels (level 1, nondiagnostic; level 2, acceptable; level 3, good; level 4, sharp); (III) display of small blood vessels, divided into four levels (level 1, small blood vessels are invisible; level 2, blood vessels are poor but still diagnostic; level 3, blood vessels are good; level 4, blood vessels are clearly visible); and (IV) overall image quality with respect to artifacts, image texture, and qualitative resolution (hereinafter referred to as overall image quality), divided into four levels (level 1, nondiagnostic; level 2, acceptable and diagnostic; level 3, good; level 4, excellent).

Evaluation of collateral circulation in reconstructed CTA

For those patients with ICA and/or MCA occlusions, a neurologist and a radiologist jointly scored and compared the collateral circulation of the six groups of CTA images according to the 6-point scoring system of Menon *et al.* (28). All the CTA images were randomized in the display order.

Statistical analysis

Statistical analysis was performed with SPSS 25.0 software (IBM Corp., Armonk, NY, USA). The quantitative data were tested for normal distribution using the Kolmogorov-Smirnov test and are expressed as mean ± SD or median with the 25th and 75th percentile, if applicable. The counting data are expressed as the number of cases and percentage. The data with normal distributions were compared with the one-way analysis of variance (ANOVA) test; Bonferroni (when the variances were equal) or Tamhane's T2 (when the variances were not equal) tests were used for the adjusted pairwise comparison. Quantitative data without normal distributions were compared using the Kruskal-Wallis test. The interagreement between the two radiologists was evaluated with the Kappa test (0.01–0.20, slight agreement; 0.21–0.40, fair agreement; 0.41–0.60, moderate agreement; 0.61–0.80, substantial agreement; 0.81–1.00, almost perfect or perfect agreement). Bland-Altman analysis with 95% limits of agreement was used to determine the concordance between CT Perfusion 4D and RAPID in the detection of

Table 1 Comparison of objective image quality of CTP images reconstructed with six different algorithms

Objective parameters	FBP	ASIR-V40%	ASIR-V80%	DLIR-L	DLIR-M	DLIR-H	F value	P value
GM								
CT value (HU)	48.62±6.18	48.59±6.11	48.57±6.16	49.46±6.09	48.56±6.20	48.52±6.03	0.014	1.000
SD (HU)	10.16±1.78	8.26±1.77†	6.57±1.61†‡	7.76±1.79†§	7.10±1.89†‡¶	6.18±1.91$^{\dagger\ddagger\S\P\#}$	104.017	<0.001
SNR	4.89±0.87	6.11±1.33†	7.78±1.93†‡	6.50±1.41†§	7.23±1.77†‡¶	8.47±2.44$^{\dagger\ddagger\S\P\#}$	91.263	<0.001
WM								
CT value (HU)	32.53±3.87	32.73±3.78	32.58±3.73	32.57±3.66	32.61±3.66	32.72±3.66	0.086	0.995
SD (HU)	9.56±1.59	7.33±1.42†	5.32±1.12†‡	6.26±1.32†‡§	5.29±1.19†‡¶	4.30±1.11$^{\dagger\ddagger\S\P\#}$	338.414	<0.001
SNR	3.49±0.67	4.62±0.98†	6.36±1.38†‡	5.41±1.19†‡§	6.45±1.53†‡¶	8.06±2.01$^{\dagger\ddagger\S\P\#}$	222.511	<0.001
CNR	1.16±0.40	1.45±0.49†	1.91±0.67†‡	1.62±0.54†§	1.84±0.63†‡¶	2.18±0.81$^{\dagger\ddagger\S\P\#}$	58.016	<0.001

Data are represented as the mean ± standard deviation. †, statistical significance with FBP, P<0.05; ‡, statistical significance with ASIR-V40%, P<0.05; §, statistical significance with ASIR-V80%, P<0.05; ¶, statistical significance with DLIR-L, P<0.05; $^{\#}$, statistical significance with DLIR-M, P<0.05. CTP, computed tomography perfusion; FBP, filtered back projection; ASIR-V, adaptive statistical iterative reconstruction-Veo; DLIR-L/M/H, deep learning-based image reconstruction at low/medium/high level; GM, gray matter; WM, white matter; HU, Hounsfield units; SD, standard deviation; SNR, signal-to-noise ratio; CNR, contrast-to-noise ratio.

ischemic core and ischemic penumbral volume. A P value <0.05 was considered statistically significant.

Results

This study enrolled 54 patients with suspected AIS, consisting of 32 males and 22 females, with an average age of 59.9±13.1 years. Among these patients, 47 were diagnosed with cerebral infarction by reexamination, 43 via MRI and 4 via NCCT. The remaining 7 patients were diagnosed with transient ischemic attack (n=4), vestibular dysfunction (n=2), or sudden hypotension shock (n=1).

The mean CTDIvol was 155.11±0.04 mGy, the mean DLP was 2,481.46±0.58 mGy·cm, and the mean ED was 5.710±0.001 mSv.

Objective image quality evaluation of CTP

There was no significant difference in CT values in the GM and WM of the frontal, temporal, and parietal lobes among the six algorithms (P_{GM}=1.000 and P_{WM}=0.995). With the increase of ASIR-V and DLIR strength, the noise decreased, while SNR, CNR, and noise reduction rates increased. The image quality of DLIR-H in terms of image noise, SNR, and CNR was significantly better than that of ASIR-V40% and 80% (all P values <0.05); however, the SD values in GM between the DLIR-H and ASIR-V80% were not significantly different (*Table 1*). No statistically significant difference in image noise, SNR, and CNR was found between ASIR-V80% and DLIR-M for both GM and WM (all P values >0.05), or between ASIR-V40% and DLIR-L in GM (all P values >0.05). The improvements in WM were more pronounced than were those in GM; nonetheless, the overall tendency was consistent (*Table 1* and *Figure 2A-2C*). Notably, DLIR-H had the highest noise reduction rate (39.7% GM; 55.1% WM) (*Figure 2D*).

Subjective image quality evaluation of CTP

The subjective scores of the five CTP pseudocolor images (for calculating CBF, CBV, Tmax, MTT, and TTP) of the six algorithms by the two radiologists were all greater than 6 points, which could meet the diagnostic requirements. Moreover, the differences were statistically significant in the overall scores of these images (P<0.001). The overall scores ranked from the lowest to highest were as follows: FBP, ASIR-V40%, DLIR-L, ASIR-V80%, DLIR-M, and DLIR-H (*Table 2* and *Figure 3*). Post hoc pairwise comparison revealed that the subjective scores of all five CTP pseudocolor images with DLIR-H, DLIR-M, and ASIR-V80% were significantly higher than those in FBP (all P values <0.05), but the differences among the DLIR-H, DLIR-M, and ASIR-V80% groups were not statistically significant. One doctor thought the subjective scores of the CTP images with DLIR-L were all higher than those in FBP, while the other doctor thought that only the subjective

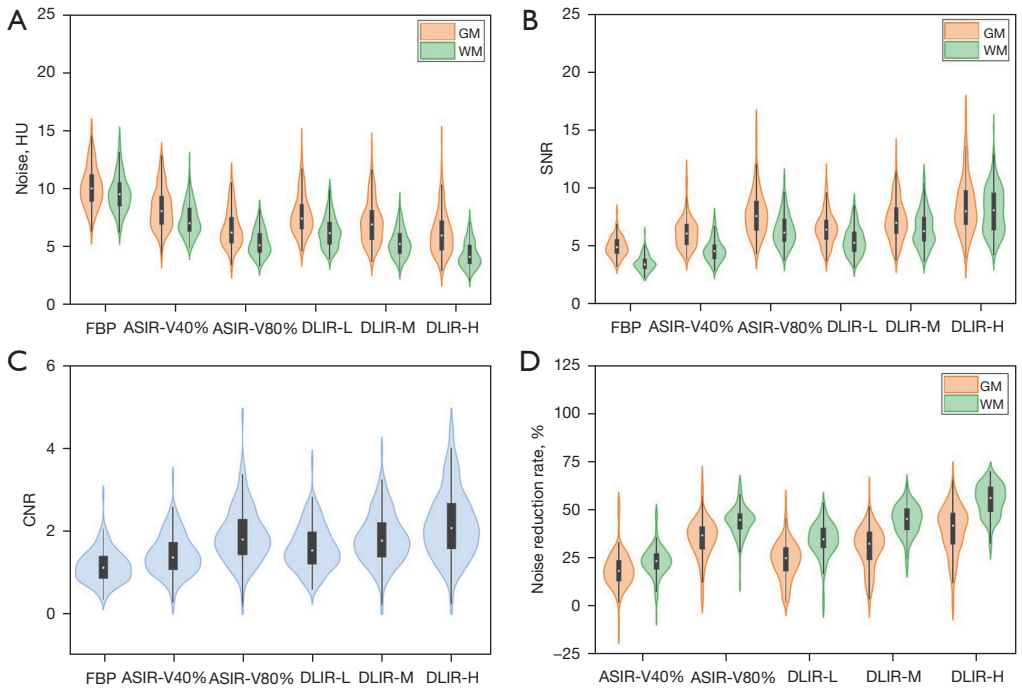

Figure 2 The objective image quality of CTP images reconstructed with FBP, ASIR-V40%, ASIR-V80%, DLIR-L, DLIR-M, and DLIR-H. (A) Noise (SD) in GM and WM. (B) SNR in GM and WM. (C) CNR in GM and WM. (D) Noise reduction rate in GM and WM. CTP, computed tomography perfusion; GM, gray matter; WM, white matter; HU, Hounsfield unit; FBP, filtered back projection; ASIR-V, adaptive statistical iterative reconstruction-Veo; DLIR-L/M/H, deep learning-based image reconstruction at low/medium/high level; SNR, signal-to-noise ratio; CNR, contrast-to-noise ratio; SD, standard deviation.

Table 2 Comparison of subjective image quality of CTP images reconstructed with six different algorithms

Perfusion parameters	FBP	ASIR-V40%	ASIR-V80%	DLIR-L	DLIR-M	DLIR-H	F value	P value
Radiologist 1								
CBF	7.13±0.87	7.52±0.67	7.76±0.51†	7.72±0.49†	7.80±0.45†	7.83±0.38†	11.294	<0.001
CBV	7.33±0.85	7.59±0.66	7.80±0.41†	7.74±0.48†	7.83±0.38†	7.81±0.39†	6.550	<0.001
Tmax	7.22±0.77	7.59±0.69†	7.80±0.45†	7.72±0.56†	7.81±0.39†	7.80±0.49†	8.552	<0.001
MTT	7.35±0.85	7.61±0.66	7.81±0.44†	7.74±0.56†	7.85±0.41†	7.78±0.46†	5.498	<0.001
TTP	6.63±1.17	7.28±0.88	7.56±0.72†	6.94±0.94†§	7.37±0.81†	7.59±0.69†¶	9.744	<0.001
Radiologist 2								
CBF	6.89±0.86	7.50±0.64†	7.59±0.63†	7.50±0.67†	7.72±0.49†	7.76±0.43†	13.365	<0.001
CBV	7.20±0.81	7.54±0.64	7.67±0.48†	7.54±0.67	7.78±0.46†	7.78±0.42†	7.065	<0.001
Tmax	7.11±0.82	7.46±0.77	7.70±0.50†	7.56±0.66†	7.74±0.48†	7.80±0.45†	8.691	<0.001
MTT	7.19±0.93	7.67±0.51	7.72±0.49†	7.50±0.80	7.80±0.56†	7.78±0.46†	6.921	<0.001
TTP	6.72±1.02	7.17±0.86	7.56±0.69†	6.98±1.02§	7.41±0.74†	7.59±0.63†¶	9.050	<0.001

Data are represented as the mean ± standard deviation. †, statistical significance with FBP, P<0.05; §, statistical significance with ASIR-V80%, P<0.05; ¶, statistical significance with DLIR-L, P<0.05. CTP, computed tomography perfusion; FBP, filtered back projection; ASIR-V, adaptive statistical iterative reconstruction-Veo; DLIR-L/M/H, deep learning-based image reconstruction at low/medium/high level; CBF, cerebral blood flow; CBV, cerebral blood volume; Tmax, time to maximum; MTT, mean transit time; TTP, time to peak.

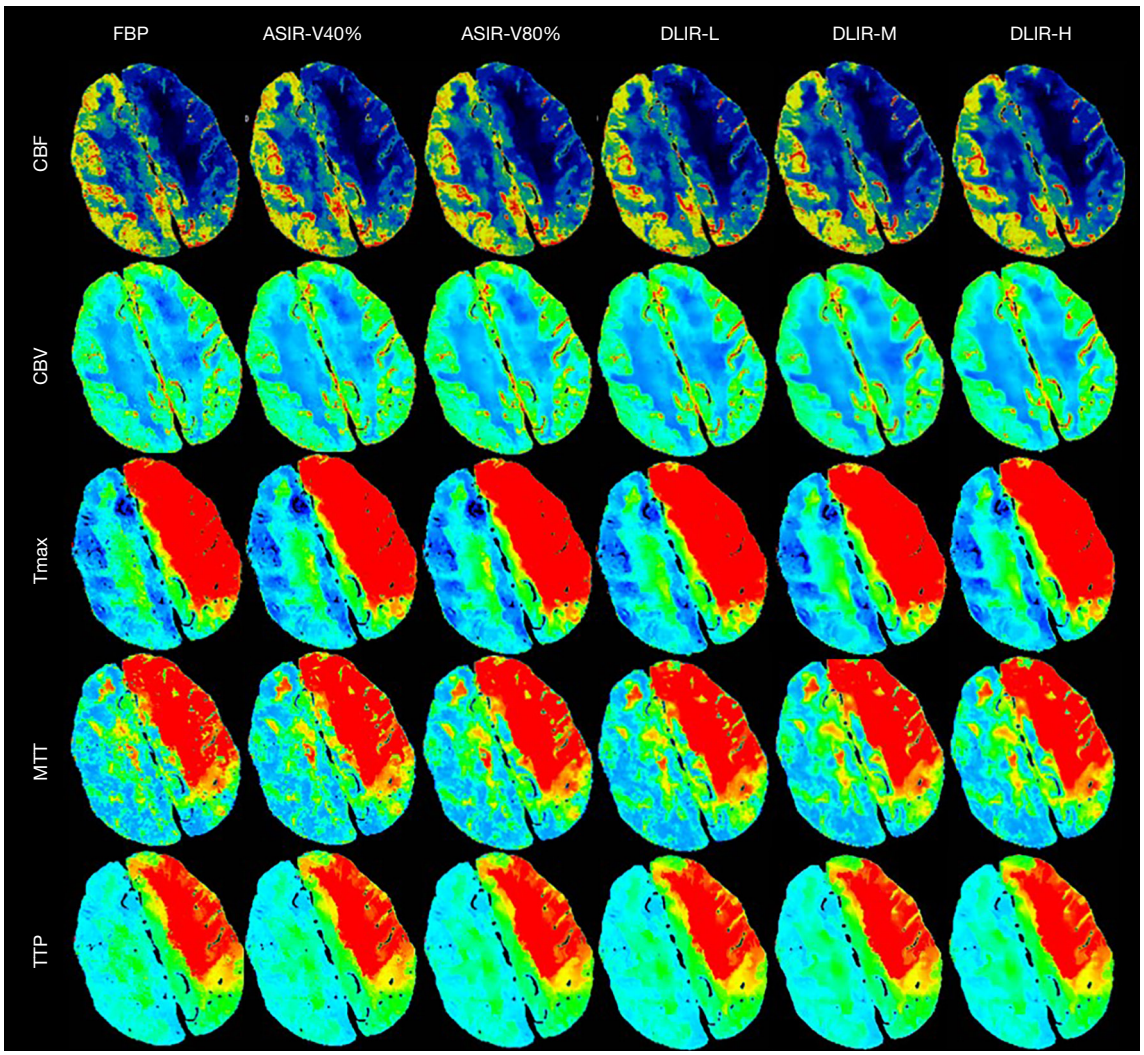

Figure 3 Perfusion maps at different reconstruction algorithms of a 59-year-old man with weakness of the right limb for 14 h. FBP, filtered back projection; ASIR-V, adaptive statistical iterative reconstruction-Veo; DLIR-L/M/H, deep learning-based image reconstruction at low/medium/high level; CBF, cerebral blood flow; CBV, cerebral blood volume; Tmax, time to maximum; MTT, mean transit time; TTP, time to peak.

scores of CBF and Tmax images in DLIR-L were higher than those in FBP (both P values <0.05). ASIR-V40% images had a higher subjective score than did the FBP images, but the scores did not differ significantly.

Interobserver agreement was substantial for CBF, CBV, Tmax, MTT, and TTP (the κ values were 0.695, 0.682, 0.656, 0.696, and 0.741 respectively) (*Figure 4*).

Evaluation of perfusion parameters

There was no significant difference in any perfusion parameters among the six algorithms for the GM or WM regions (*Table 3*). The values of CBF and CBV in GM were significantly higher than those in WM, while those of Tmax, MTT, and TTP were smaller.

In a comparison of the perfusion parameters from the six groups of images automatically calculated with CT Perfusion 4D, no significant difference was found in the infarct core, tissue at risk, or ischemic penumbra (P>0.05), and the same was true for RAPID. The detection accuracy of AIS on CTP was 89.4% with DLIR-H, 87.2% with DLIR-M, and 83.0% with FBP, ASIR-V40%, ASIR-V80%, and DLIR-L (*Table 4*). The Bland-Altman analysis showed that the mean differences in ischemic core between CT

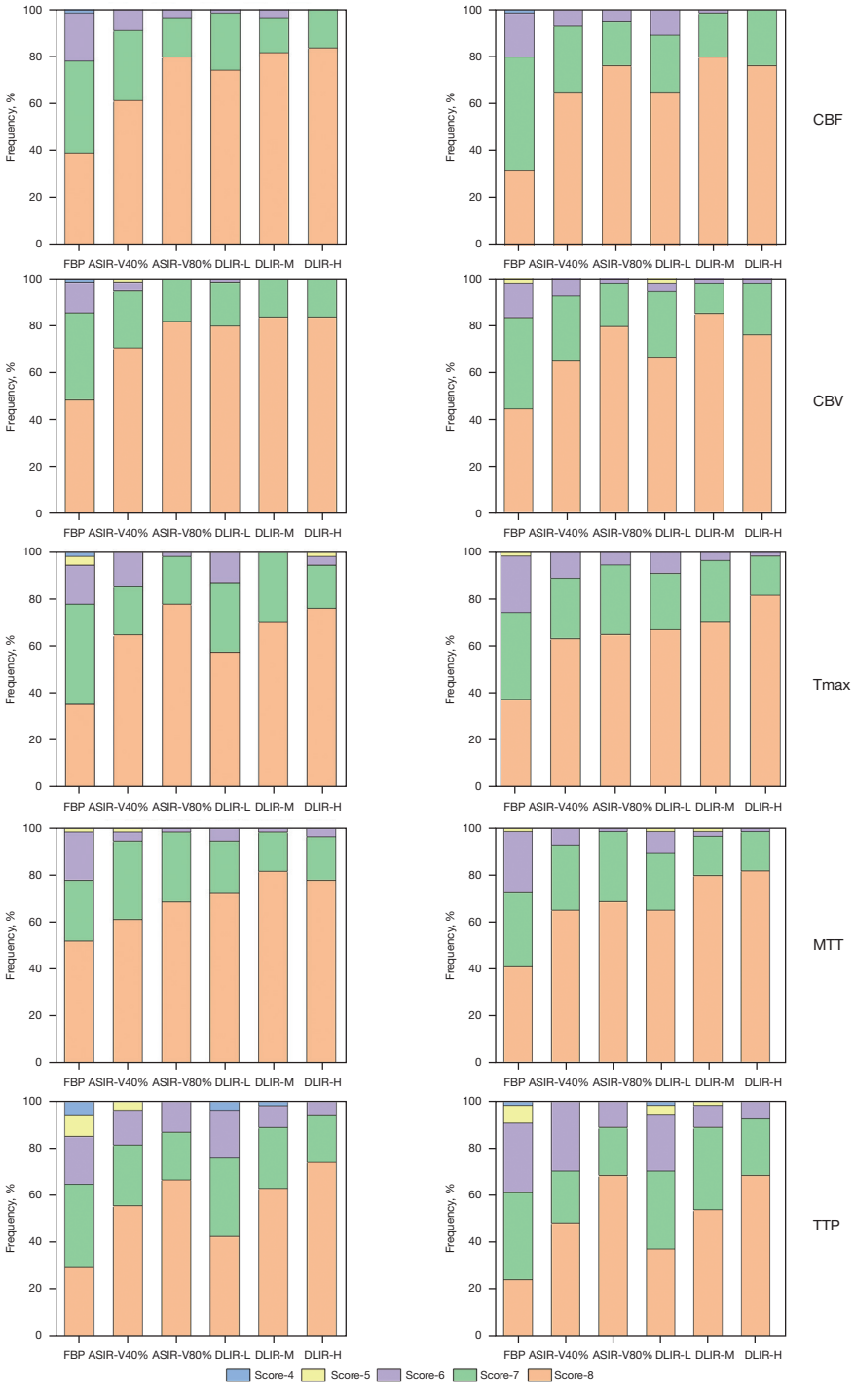

Figure 4 Stacked bar graph with ratings for overall subjective image quality scores of all CTP images by two radiologists (8-point score; >6, high quality and diagnostic value; 3–6, medium quality but still sufficient for diagnosis; <3, poor and insufficient for diagnosis). The Kappa (κ) values between the 2 radiologists were 0.695 for CBF, 0.682 for CBV, 0.656 for Tmax, 0.696 for MTT, and 0.741 for TTP. FBP, filtered back projection; ASIR-V, adaptive statistical iterative reconstruction-Veo; DLIR-L/M/H, deep learning–based image reconstruction at low/medium/high level; CBF, cerebral blood flow; CBV, cerebral blood volume; Tmax, time to maximum; MTT, mean transit time; TTP, time to peak; CTP, computed tomography perfusion.

Table 3 Comparison of perfusion parameters of CTP images reconstructed with six different algorithms

Perfusion parameters	FBP	ASIR-V40%	ASIR-V80%	DLIR-L	DLIR-M	DLIR-H	F value	P value
GM								
CBF (mL/100 g/min)	49.11±15.93	49.02±18.77	48.91±16.13	48.86±16.49	48.92±16.56	49.02±16.00	0.005	1.000
CBV (mL/100 g)	2.52±0.51	2.55±0.59	2.51±0.49	2.56±0.46	2.55±0.48	2.57±0.49	0.263	0.933
Tmax (s)	2.74±0.98	2.74±0.97	2.72±0.98	2.74±0.93	2.73±0.93	2.72±0.93	0.015	1.000
MTT (s)	3.70±1.73	3.75±1.71	3.69±1.68	3.75±1.49	3.72±1.63	3.66±1.53	0.074	0.996
TTP (s)	12.50±1.71	12.38±1.60	12.42±1.63	12.39±1.61	12.34±1.68	12.40±1.72	0.166	0.975
WM								
CBF (mL/100 g/min)	13.73±5.77	13.51±6.40	13.08±5.41	14.20±5.98	13.94±6.37	14.03±6.05	0.761	0.578
CBV (mL/100 g)	1.30±0.32	1.32±0.37	1.31±0.31	1.33±0.30	1.32±0.31	1.34±0.33	0.320	0.901
Tmax (s)	4.02±1.16	4.00±1.15	4.04±1.15	4.06±1.20	4.04±1.17	4.05±1.19	0.109	0.990
MTT (s)	7.08±2.57	7.06±2.48	7.17±2.49	6.87±2.66	6.98±2.69	6.93±2.68	0.290	0.919
TTP (s)	13.70±1.73	13.55±1.61	13.59±1.63	13.61±1.62	13.62±1.67	13.62±1.67	0.145	0.981

Data are represented as mean ± standard deviation. CTP, computed tomography perfusion; FBP, filtered back projection; ASIR-V, adaptive statistical iterative reconstruction-Veo; DLIR-L/M/H, deep learning-based image reconstruction at low/medium/high level; GM, gray matter; WM, white matter; CBF, cerebral blood flow; CBV, cerebral blood volume; Tmax, time to maximum; MTT, mean transit time; TTP, time to peak.

Perfusion 4D and RAPID was 1.24 mL while the mean differences in ischemic penumbra between CT Perfusion 4D and RAPID was 2.59 mL based on DLIR-H CTP images (*Figure 5*).

Objective image quality evaluation of the CTA reconstruction

Among the CTA images of all six groups, CT values of the ICA siphons, MCA-M1, and temporalis showed no statistical significance, and there was also no statistically significant difference in the noise or SNR of MCA-M1; meanwhile, the while noise and SNR of the ICA siphons and temporalis, as well as the CNR of the ICA siphons and MCA-M1, were statistically significant (all P values <0.05). In addition, noise, SNR, and CNR were comparable among the DLIR-M, DLIR-H, and ASIR-V80% groups, with DLIR-H images showing better quality compared to the DLIR-M and ASIR-V80% images. The noise of the temporalis in CTA images reconstructed with DLIR-L was higher than that in images reconstructed with DLIR-H, and the SNR was lower (P<0.05). The noise of CTA images with FBP was the highest, while SNR and CNR were the lowest (*Table 5*).

Subjective image quality evaluation of the CTA reconstruction

There were significant differences in image noise, edge sharpness of the vascular lumen, display of small blood vessels, and overall image quality among the six groups of CTA images (P<0.05; *Figures 6*,*7*). The subjective scores of the DLIR-H and DLIR-M images were the highest. The CTA images with ASIR-V80% were slightly inferior to those with DLIR-M and DLIR-H in image noise and overall image quality (P<0.05), but there was no significant difference in the edge sharpness of the vascular lumen or the display of small blood vessels among the three groups. The subjective grading of CTA images in FBP and ASIR-V40% were lower than those of the other four groups (P<0.05), but there was no statistical difference between the FBP and ASIR-V40% groups (P>0.05).

Evaluation of collateral circulation in CTA reconstruction

There were 38 patients with ICA and/or MCA occlusions. The collateral circulation scores of the six reconstructed CTA images for each patient were all consistent (*Figure 6*).

Table 4 Comparison of perfusion parameters related to cerebral infarction of CTP images reconstructed with six different algorithms

Perfusion parameters	FBP	ASIR-V40%	ASIR-V80%	DLIR-L	DLIR-M	DLIR-H	H value	P value
Tissue at risk (mL)								
Perf. 4D							0.016	1.000
Mean ± SD	102.95±87.80	103.23±89.08	104.49±90.61	102.87±87.73	103.04±90.09	104.19±90.34		
Median (P25, P75)	93.70 (14.50, 156.25)	94.00 (14.10, 147.50)	100.00 (15.09, 159.25)	95.50 (14.63, 155.50)	95.00 (14.43, 156.25)	101.00 (14.89, 159.5)		
RAPID							0.201	0.999
Mean ± SD	105.40±88.10	105.88±89.19	103.68±88.17	103.56±89.08	102.34±89.26	101.60±89.22		
Median (P25, P75)	104.00 (13.50, 160.50)	102.50 (13.00, 159.50)	98.50 (12.00, 157.25)	96.00 (14.25, 157.50)	93.50 (9.25, 155.25)	91.50 (11.25, 153.25)		
Ischemic core (mL)								
Perf. 4D							0.325	0.997
Mean ± SD	16.20±40.98	15.90±40.64	16.27±41.13	16.18±39.31	16.38±40.7	16.52±40.20		
Median (P25, P75)	4.90 (0, 17.42)	4.51 (0, 19)	4.62 (0.03, 21.25)	4.45 (0.04, 18.75)	4.19 (0.03, 19.5)	4.93 (0, 22.75)		
RAPID							0.008	1.000
Mean ± SD	17.68±45.05	17.82±45.01	17.48±45.02	17.88±45.32	17.74±45.48	17.76±45.35		
Median (P25, P75)	5 (0, 16.50)	4 (0, 17.75)	5 (0, 16.50)	4 (0, 16.50)	5 (0, 16)	5 (0, 17)		
Mismatch volume (mL)								
Perf. 4D							0.024	1.000
Mean ± SD	86.74±68.71	87.33±69.44	88.21±70.99	86.69±68.10	86.66±70.11	87.67±70.76		
Median (P25, P75)	91.42 (14.16, 128.13)	93.23 (14.11, 130.50)	94.82 (15.09, 127.25)	88.73 (14.47, 127)	85.10 (14.43, 131.25)	80.39 (14.62, 128.25)		
RAPID							0.281	0.998
Mean ± SD	87.72±69.18	88.06±69.89	86.20±69.29	85.68±69.44	84.60±69.57	83.84±69.18		
Median (P25, P75)	88.50 (13.50, 135.00)	90.50 (13.00, 139.00)	87.50 (12.00, 135.25)	84.50 (14.25, 134.75)	78.50 (9.25, 135.5)	79.00 (11.25, 132.75)		
Detection rate, % (proportion)	83.0 (39/47)	83.0 (39/47)	83.0 (39/47)	83.0 (39/47)	87.2 (41/47)	89.4 (42/47)		

CTP, computed tomography perfusion; FBP, filtered back projection; ASIR-V, adaptive statistical iterative reconstruction-Veo; DLIR-L/M/H, deep learning–based image reconstruction at low/medium/high level; Perf.4D, CT Perfusion 4D software of the Advantage Workstation 4.7 (GE HealthCare); RAPID, Rapid Processing of Perfusion and Diffusion (ISchemiaView Inc.); SD, standard deviation.

Discussion

In this study, the image quality of CTP images and the reconstructed CTA images at the peak arterial phase, perfusion parameters, and diagnostic accuracy for AIS under six reconstruction algorithms (FBP, ASIR-V40%, ASIR-V80%, DLIR-L, DLIR-M, and DLIR-H) in patients with suspected AIS were evaluated. Results showed that the objective and subjective quality of CTP images and CTA images reconstructed by DLIR-H and DLIR-M were superior to those of the routine advanced ASIR-V40% algorithm and traditional FBP algorithm. As for the diagnostic performance for acute cerebral infarction, DLIR-H had the highest detection accuracy. The CT Perfusion 4D and RAPID software showed good agreement on diagnostic agreements and assessments of tissue at risk, ischemic core, and ischemic penumbra based on DLIR-H.

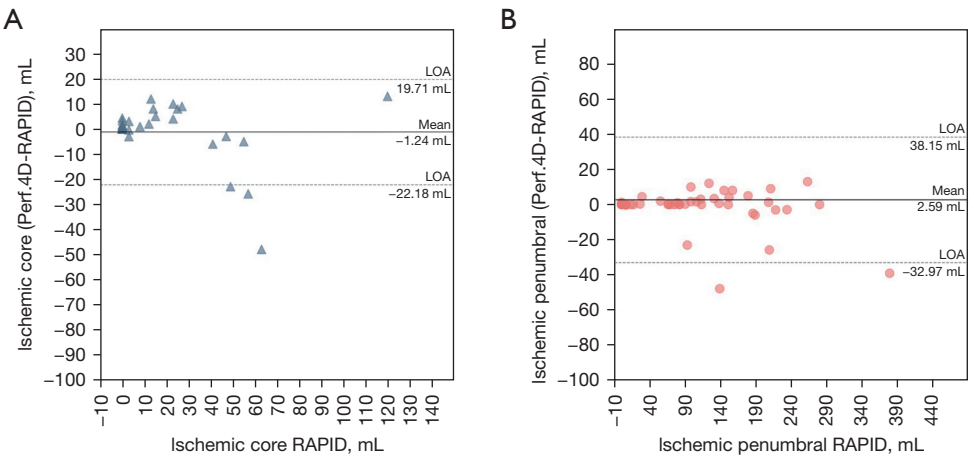

Figure 5 Bland-Altman plots of agreement in the (A) volumes of ischemic cores and (B) volumes of ischemic penumbra between Perf.4D and RAPID software. Solid lines demonstrate the mean difference from the RAPID software. Dotted lines represent 95% LOA. Perf.4D, CT Perfusion 4D software of the Advantage Workstation 4.7 (GE HealthCare); RAPID, Rapid Processing of Perfusion and Diffusion (ISchemiaView Inc.); LOA, limits of agreement.

Table 5 Comparison of objective image quality images of CTP arterial peak phase reconstructed with six different algorithms

Objective parameters	FBP	ASIR-V40%	ASIR-V80%	DLIR-L	DLIR-M	DLIR-H	F value	P value
SD value								
ICA siphon	31.43±7.95	29.99±8.23	28.70±8.59	27.29±6.68	26.25±6.84	25.48±7.07†	3.253	0.008
Temporalis	18.80±4.25	14.44±3.88†	10.49±3.80†‡	13.66±3.64†§	12.05±3.56†	10.58±3.53†‡¶	24.402	<0.001
SNR								
ICA siphon	18.55±6.47	19.58±6.96	20.65±7.52	21.01±5.44	21.99±5.84	22.90±6.37	2.842	0.042
Temporalis	3.02±1.43	4.03±1.99	5.85±3.10†‡	4.17±1.53†§	4.81±1.80†	5.59±2.19†‡¶	9.507	<0.01
CNR								
ICA siphon	14.06±4.86	15.58±5.48	17.15±6.20†	16.56±4.38†	17.51±4.51†	18.43±4.71†‡	3.364	<0.01
MCA-M1	11.77±3.62	12.63±3.76	13.02±4.71†	13.16±4.15†	13.72±4.62†	14.93±5.20†‡	3.512	<0.01

Data are represented as the mean ± SD. †, statistical significance with FBP, P<0.05; ‡, statistical significance with ASIR-V40%, P<0.05; §, statistical significance with ASIR-V80%, P<0.05; ¶, statistical significance with DLIR-L, P<0.05. CTP, computed tomography perfusion; FBP, filtered back projection; ASIR-V, adaptive statistical iterative reconstruction-Veo; DLIR-L/M/H, deep learning-based image reconstruction at low/medium/high level; SD, standard deviation; SNR, signal-to-noise ratio; CNR, contrast-to-noise ratio; ICA siphon, siphon of the internal carotid artery; MCA-M1, M1 segment of the middle cerebral artery.

CT examinations are essential for the early diagnosis and treatment of neurological diseases. Studies have proven that DLIR provides better image quality than does the IR algorithm in brain NCCT scans (21,29,30). In our study, we confirmed that DLIR-H and DLIR-M, as compared with ASIR-V and FBP, could achieve better image quality without changing the CT values and perfusion parameters on whole-brain CTP. Specifically, DLIR had lower image noise, and higher SNR, CNR, and noise reduction rate than did ASIR-V and FBP. Furthermore, we also found that the image improvement of DLIR in noise, SNR, and noise reduction rate of WM was more sensitive than that of GM, which may be due to the fact that GM is the place neurons are concentrated, while WM is mainly composed of nerve fibers; these results are in line with those of brain NCCT reported by Sun *et al.* (31). We additionally

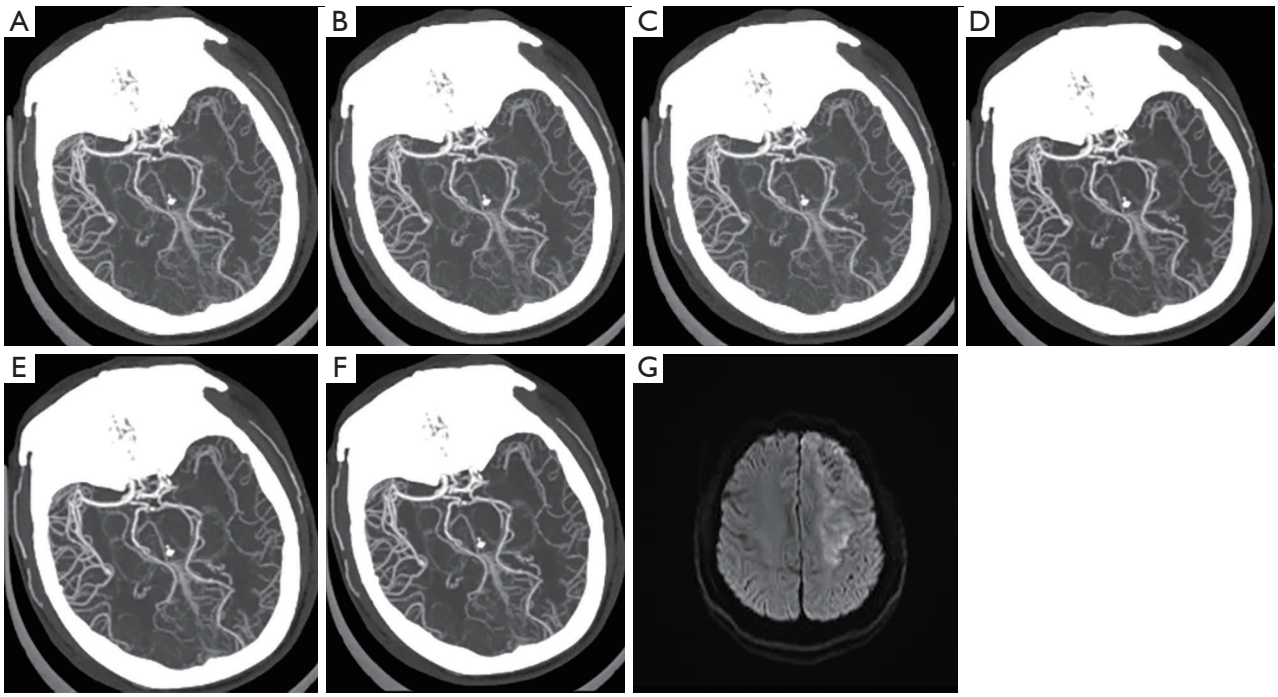

Figure 6 The images of the CTP arterial peak phase reconstructed with different algorithms (A-F) and the MRI image reviewed after treatment (G) from the same patient as in *Figure 4*. (A-F) The images of CTP arterial peak phase reconstructed with the FBP, ASIR-V40%, ASIR-V80%, DLIR-L, DLIR-M, and DLIR-H algorithms, respectively. CTP, computed tomography perfusion; MRI, magnetic resonance imaging; FBP, filtered back projection; ASIR-V, adaptive statistical iterative reconstruction-Veo; DLIR-L/M/H, deep learning-based image reconstruction at low/medium/high level.

conducted subjective assessments with a 3-point scoring system for CTP assessment described by Abels *et al.* (25). Notably, we noticed that the subjective scores of TTP maps reconstructed with DLIR-L were lower than those reconstructed with ASIR-V40%, as assessed by radiologist 1 and radiologist 2. However, all assessments based on CTP maps reconstructed with DLIR-H and DLIR-M, including CBF, CBV, Tmax, MTT, and TTP, achieved scores higher than those of FBP and ASIR-V40%. Overall, DLIR-H had the best performance among the six groups. Therefore, we recommend using the DLIR-H algorithm for image reconstruction of cerebral CTP examination. The subjective score of CTP images in DLIR-H and DLIR-M was higher than that of ASIR-V40% and was in line with two studies that examined brain nonenhanced CT (21,30), both of which compared the ASIR-V50% with DLIR.

Furthermore, we compared the diagnostic agreement for the volume of ischemic core and penumbra estimated via CT Perfusion 4D and RAPID software. Consistent with previous research (26,32), we found that CT Perfusion 4D showed excellent concordance with RAPID for quantifying ischemic core volume and penumbra. Moreover, we assessed the diagnostic performance of CTP reconstructed with six reconstruction algorithms, and the results for core infarct lesion detection showed that CTP images reconstructed with DLIR-H had the highest diagnostic accuracy, which is in agreement with the lesion detection results from the brain nonenhanced CT study of Sun *et al.* (31). In their study, they found that thin-slice, 0.625-mm thick images from DLIR-H were more sensitive in detecting small hemorrhagic lesions compared with DLIR-L. In our study, CTP with DLIR-M and DLIR-H detected 41 and 42 lesions out of the total 47 lesions, two and three more than the other reconstruction algorithms, respectively. The two additional lesions detected with DLIR-M and DLIR-H were located in the left occipital lobe, and the extra 1 detected by DLIR-H alone was located in the left corona radiata. We inferred that the improvement of the detection accuracy for small lesions could be attributed to the higher low-contrast detectability of DLIR (17). We are looking forward to conducting subsequent studies that include a greater number of small infarct lesions to further

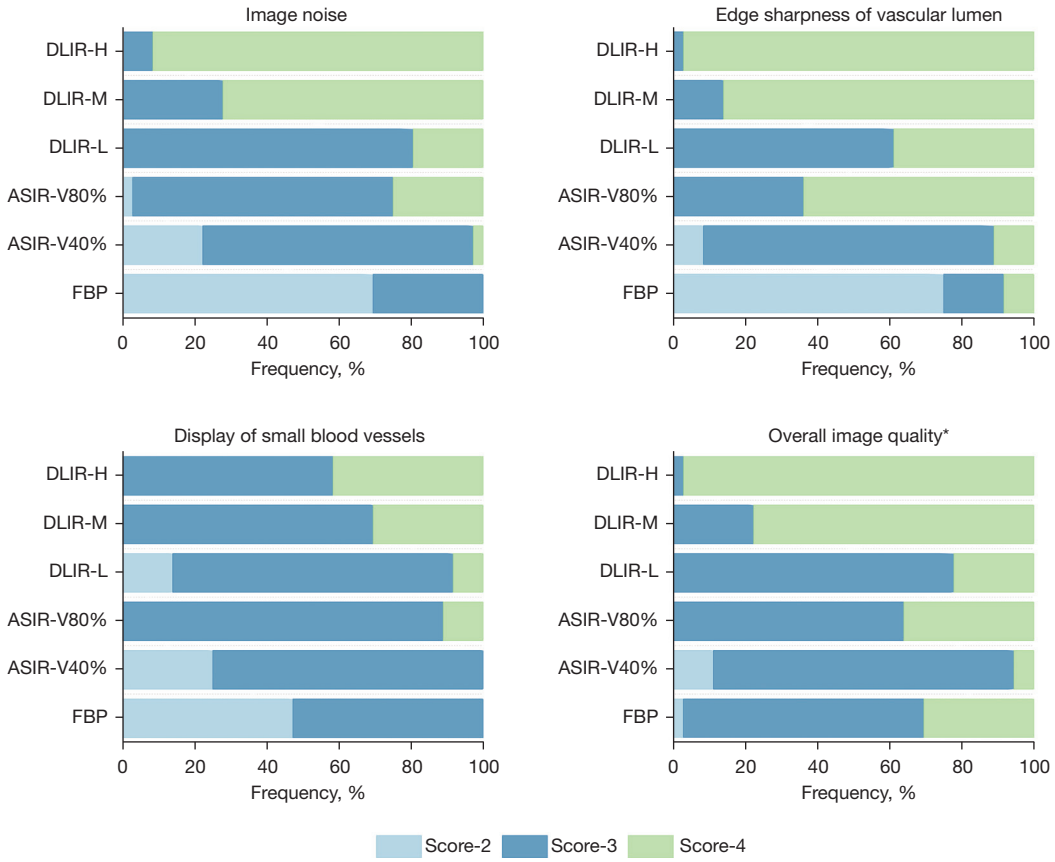

Figure 7 Subjective scores of images of CTP arterial peak phase reconstructed with 6 different algorithms. *, overall image quality with respect to artifacts, image texture, and qualitative resolution. DLIR-L/M/H, deep learning–based image reconstruction at low/medium/high level; ASIR-V, adaptive statistical iterative reconstruction-Veo; FBP, filtered back projection; CTP, computed tomography perfusion.

confirm the detectability improvement of DLIR for small lesions. Particularly, we noticed that in previous studies, CTP was less sensitive to the detection of lacunar infarction compared with MRI (33,34). The inherently low CNR of CTP pseudocolor images makes it difficult to identify small infarct cores visually under high background noise (35). Partial volume effect and the mixing of diseased tissues with adjacent normal tissues could also lead to the omission of small lesions (36). Hana *et al.* found that the sensitivity of CTP was higher when the infarct area was more than 3 cm^2 (83% *vs.* 29%; P<0.001) (37). In our study, five lesions were confirmed by MRI but missed by CTP, of which two of were located in the brainstem, one in the occipital lobe, and two in the frontal lobe. Therefore, although the diagnostic accuracy of CTP images reconstructed with DLIR for cerebral infarction was improved to some extent, for such relatively small lesions, higher-resolution CT images are needed to achieve the same diagnostic level as that of MRI.

Vessel imaging in diagnosing patients with AIS is also crucial. In our study, vessel imaging (CTA) was realized by reconstructing the CTP datasets acquired at the peak arterial phase to reduce the radiation dose. The objective image quality of CTA images reconstructed with DLIR-H and DLIR-M was higher as compared to ASIR-V40% and were on par or better as compared to ASIR-V80%. The noise reduction in the temporalis was more obvious than that in the intracranial blood vessels, especially the MCA. The overall quality of CTA images in the DLIR-H and DLIR-M groups was rated the best. Therefore, in contrast to the conventional scan protocol of performing CTA separately, reconstruction of intracranial CTA images from CTP may be a novel strategy for reducing radiation and contrast agent dose in patients with AIS. However, a recent study by Chen *et al.* (38) showed that the CT value

of ICA siphons in the peak arterial phase images of CTP reconstructed with the advanced intelligent clear IQ engine (AiCE) based on deep learning was higher than that of the 3D adaptive iterative dose reduction (AIDR 3D) algorithm, with the image noise value being higher and the SNR lower. This may attributable to the different principles of developing deep learning algorithms from different manufacturers. Further research is needed to verify the differences among the various commercially available deep learning-based algorithms.

Our study has several limitations. First, the number of patients with AIS included in our study was limited, and a greater number of cases are expected for further studies. Second, this study only evaluated two strength levels (40% and 80% levels) for ASIR-V, and other reconstruction strengths were not included. However, ASIR-V40% and ASIR-V80% are the two commonly used algorithms clinically, representing the medium and high strength reconstructions, respectively. In addition, our pre-experiments showed that there was no significant difference in image quality between our routine ASIR-V40% and the ASIR-V50% used by others. Third, the exact time of onset for some patients with cerebral infarction was unknown, and we excluded them from enrollment for the authenticity of this study, which might have resulted in biasing of the data. Finally, the radiation dose of CTP was also of considerable concern, but we did not lower the dose for examination in this study, and this may be another direction of research in DLIR application.

In summary, compared with the FBP algorithm and the ASIR-V algorithm with medium strength, the DLIR-H and DLIR-M algorithms significantly improved both the subjective and objective image quality of CTP and CTA derived from the CTP peak artery phase. The overall image quality of DLIR-H and DLIR-M was basically comparable or superior to that of ASIR-V80%. DLIR-H also improved the detection accuracy of cerebral infarction lesions. In addition, intracranial CTA images reconstructed from CTP could further reduce the dosage of contrast agents and radiation.

Acknowledgments

We would like to thank Dr. Lirong Chao (GE HealthCare) for his help in setting up the scanning protocol. Parts of the manuscript have been presented as a poster presentation at the Radiological Society of North America (RSNA) 2022 annual meeting.

Funding: This work was supported by the Key Science and Technology Program of Henan Province, China (No. 232102310098).

Footnote

Conflicts of Interest: All authors have completed the ICMJE uniform disclosure form (available at https://qims.amegroups.com/article/view/10.21037/qims-23-547/coif). LW is an employee of GE HealthCare, the manufacturer of the CT system used in this study. The other authors have no conflicts of interest to declare.

Ethical Statement: The authors are accountable for all aspects of the work in ensuring that questions related to the accuracy or integrity of any part of the work are appropriately investigated and resolved. The study was conducted in accordance with the Declaration of Helsinki (as revised in 2013) and was approved by the Human Research Ethics Committee of the First Affiliated Hospital of Zhengzhou University (No. 2022-KY-0929-002). All enrolled patients signed written informed consent forms.

References

1. Virani SS, Alonso A, Aparicio HJ, Benjamin EJ, Bittencourt MS, Callaway CW, et al. Heart Disease and Stroke Statistics-2021 Update: A Report From the American Heart Association. Circulation 2021;143:e254-743.
2. Nogueira RG, Jadhav AP, Haussen DC, Bonafe A, Budzik RF, Bhuva P, et al. Thrombectomy 6 to 24 Hours after Stroke with a Mismatch between Deficit and Infarct. N Engl J Med 2018;378:11-21.
3. Albers GW, Marks MP, Kemp S, Christensen S, Tsai JP, Ortega-Gutierrez S, et al. Thrombectomy for Stroke at 6 to 16 Hours with Selection by Perfusion Imaging. N Engl J Med 2018;378:708-18.
4. Lu Q, Fu J, Lv K, Han Y, Pan Y, Xu Y, Zhang J, Geng D.

Agreement of three CT perfusion software packages in patients with acute ischemic stroke: A comparison with RAPID. Eur J Radiol 2022;156:110500.
5. Mokin M, Levy EI, Saver JL, Siddiqui AH, Goyal M, Bonafé A, Cognard C, Jahan R, Albers GW; SWIFT PRIME Investigators. Predictive Value of RAPID Assessed Perfusion Thresholds on Final Infarct Volume in SWIFT PRIME (Solitaire With the Intention for Thrombectomy as Primary Endovascular Treatment). Stroke 2017;48:932-8.
6. Gallissot F, Lenfant M, Thouant P, Haioun K, Thay A, Ricolfi F, Comby PO. Temporal averaging angiographic reconstructions from whole-brain CT perfusion for the detection of vasospasm. J Neuroradiol 2023;50:333-40.
7. Lu SS, Zhang X, Xu XQ, Cao YZ, Zhao LB, Liu QH, Wu FY, Liu S, Shi HB. Comparison of CT angiography collaterals for predicting target perfusion profile and clinical outcome in patients with acute ischemic stroke. Eur Radiol 2019;29:4922-9.
8. Niesten JM, van der Schaaf IC, Riordan AJ, de Jong HW, Horsch AD, Eijspaart D, Smit EJ, Mali WP, Velthuis BK. Radiation dose reduction in cerebral CT perfusion imaging using iterative reconstruction. Eur Radiol 2014;24:484-93.
9. Othman AE, Brockmann C, Yang Z, Kim C, Afat S, Pjontek R, Nikoubashman O, Brockmann MA, Kim JH, Wiesmann M. Effects of radiation dose reduction in Volume Perfusion CT imaging of acute ischemic stroke. Eur Radiol 2015;25:3415-22.
10. Manniesing R, Oei MT, van Ginneken B, Prokop M. Quantitative Dose Dependency Analysis of Whole-Brain CT Perfusion Imaging. Radiology 2016;278:190-7.
11. Othman AE, Afat S, Brockmann C, Nikoubashman O, Bier G, Brockmann MA, Nikolaou K, Tai JH, Yang ZP, Kim JH, Wiesmann M. Low-Dose Volume-Perfusion CT of the Brain: Effects of Radiation Dose Reduction on Performance of Perfusion CT Algorithms. Clin Neuroradiol 2017;27:311-8.
12. Geyer LL, Schoepf UJ, Meinel FG, Nance JW Jr, Bastarrika G, Leipsic JA, Paul NS, Rengo M, Laghi A, De Cecco CN. State of the Art: Iterative CT Reconstruction Techniques. Radiology 2015;276:339-57.
13. Koetzier LR, Mastrodicasa D, Szczykutowicz TP, van der Werf NR, Wang AS, Sandfort V, van der Molen AJ, Fleischmann D, Willemink MJ. Deep Learning Image Reconstruction for CT: Technical Principles and Clinical Prospects. Radiology 2023;306:e221257.
14. Zhu Z, Zhao Y, Zhao X, Wang X, Yu W, Hu M, Zhang X, Zhou C. Impact of preset and postset adaptive statistical iterative reconstruction-V on image quality in nonenhanced abdominal-pelvic CT on wide-detector revolution CT. Quant Imaging Med Surg 2021;11:264-75.
15. Li K, Tang J, Chen GH. Statistical model based iterative reconstruction (MBIR) in clinical CT systems: experimental assessment of noise performance. Med Phys 2014;41:041906.
16. Singh S, Kalra MK, Gilman MD, Hsieh J, Pien HH, Digumarthy SR, Shepard JA. Adaptive statistical iterative reconstruction technique for radiation dose reduction in chest CT: a pilot study. Radiology 2011;259:565-73.
17. Hsieh J, Liu E, Nett B, Tang J, Sahney S. A new era of image reconstruction: TrueFidelityTM, Technical white paper on deep learning image reconstruction. GE HealthCare 2020. Available online: https://www.semanticscholar.org/paper/A-new-era-of-image-reconstruction%3A-TrueFidelityTM-Hsieh-Liu/d0f8e1e8868e9f8ed22ad5972420139551552e91
18. Greffier J, Hamard A, Pereira F, Barrau C, Pasquier H, Beregi JP, Frandon J. Image quality and dose reduction opportunity of deep learning image reconstruction algorithm for CT: a phantom study. Eur Radiol 2020;30:3951-9.
19. Benz DC, Ersözlü S, Mojon FLA, Messerli M, Mitulla AK, Ciancone D, Kenkel D, Schaab JA, Gebhard C, Pazhenkottil AP, Kaufmann PA, Buechel RR. Radiation dose reduction with deep-learning image reconstruction for coronary computed tomography angiography. Eur Radiol 2022;32:2620-8.
20. Jiang B, Li N, Shi X, Zhang S, Li J, de Bock GH, Vliegenthart R, Xie X. Deep Learning Reconstruction Shows Better Lung Nodule Detection for Ultra-Low-Dose Chest CT. Radiology 2022;303:202-12.
21. Kim I, Kang H, Yoon HJ, Chung BM, Shin NY. Deep learning-based image reconstruction for brain CT: improved image quality compared with adaptive statistical iterative reconstruction-Veo (ASIR-V). Neuroradiology 2021;63:905-12.
22. Yao Y, Guo B, Li J, Yang Q, Li X, Deng L. The influence of a deep learning image reconstruction algorithm on the image quality and auto-analysis of pulmonary nodules at ultra-low dose chest CT: a phantom study. Quant Imaging Med Surg 2022;12:2777-91.
23. Flottmann F, Kabath J, Illies T, Schneider T, Buhk JH, Fiehler J, Kemmling A. Iterative Reconstruction Improves Both Objective and Subjective Image Quality in Acute Stroke CTP. PLoS One 2016;11:e0150103.
24. Wintermark M, Maeder P, Verdun FR, Thiran JP, Valley JF, Schnyder P, Meuli R. Using 80 kVp versus 120 kVp

in perfusion CT measurement of regional cerebral blood flow. AJNR Am J Neuroradiol 2000;21:1881-4.
25. Abels B, Klotz E, Tomandl BF, Villablanca JP, Kloska SP, Lell MM. CT perfusion in acute ischemic stroke: a comparison of 2-second and 1-second temporal resolution. AJNR Am J Neuroradiol 2011;32:1632-9.
26. Lee TY, Chung K, De Sarno D, Galas T, Adam V, Bonnard M, Deubig A, Sirohey S. Tissue Segmentation in Acute Ischemic Stroke. GE HealthCare 2022. Available online: https://www.gehealthcare.com/
27. Campbell BCV, Mitchell PJ, Churilov L, Yassi N, Kleinig TJ, Dowling RJ, et al. Tenecteplase versus Alteplase before Thrombectomy for Ischemic Stroke. N Engl J Med 2018;378:1573-82.
28. Menon BK, d'Esterre CD, Qazi EM, Almekhlafi M, Hahn L, Demchuk AM, Goyal M. Multiphase CT Angiography: A New Tool for the Imaging Triage of Patients with Acute Ischemic Stroke. Radiology 2015;275:510-20.
29. Oostveen LJ, Meijer FJA, de Lange F, Smit EJ, Pegge SA, Steens SCA, van Amerongen MJ, Prokop M, Sechopoulos I. Deep learning-based reconstruction may improve non-contrast cerebral CT imaging compared to other current reconstruction algorithms. Eur Radiol 2021;31:5498-506.
30. Alagic Z, Diaz Cardenas J, Halldorsson K, Grozman V, Wallgren S, Suzuki C, Helmenkamp J, Koskinen SK. Deep learning versus iterative image reconstruction algorithm for head CT in trauma. Emerg Radiol 2022;29:339-52.
31. Sun J, Li H, Wang B, Li J, Li M, Zhou Z, Peng Y. Application of a deep learning image reconstruction (DLIR) algorithm in head CT imaging for children to improve image quality and lesion detection. BMC Med Imaging 2021;21:108.
32. Liu QC, Jia ZY, Zhao LB, Cao YZ, Ma G, Shi HB, Liu S. Agreement and Accuracy of Ischemic Core Volume Evaluated by Three CT Perfusion Software Packages in Acute Ischemic Stroke. J Stroke Cerebrovasc Dis 2021;30:105872.
33. Chen P, G. L, Lu C, Chen S, Hui J, Zhao Z, Ji J. Diagnostic value of low dose dual-source CT cerebral perfusion imaging in patients with hyperacute cerebral infarction. Chinese Journal of Radiology 2020;54:112-8.
34. Abdelgawad EA, Higazi MM, Abdelbaky AO, Abdelghany HS. Diagnostic performance of CT cerebral blood volume colour maps for evaluation of acute infarcts; comparison with diffusion-weighted MRI within 12hours of major stroke onset. J Neuroradiol 2017;44:10-6.
35. González RG. Low signal, high noise and large uncertainty make CT perfusion unsuitable for acute ischemic stroke patient selection for endovascular therapy. J Neurointerv Surg 2012;4:242-5.
36. Lin L, Bivard A, Parsons MW. Perfusion patterns of ischemic stroke on computed tomography perfusion. J Stroke 2013;15:164-73.
37. Hana T, Iwama J, Yokosako S, Yoshimura C, Arai N, Kuroi Y, Koseki H, Akiyama M, Hirota K, Ohbuchi H, Hagiwara S, Tani S, Sasahara A, Kasuya H. Sensitivity of CT perfusion for the diagnosis of cerebral infarction. J Med Invest 2014;61:41-5.
38. Chen Y, Wang Y, Su T, Xu M, Yan J, Wang J, lu X, Wang Y, Li Y, Jin Z. The preliminary results of the effect of deep learning-based reconstruction on cerebral CT perfusion: cerebral parameters and image quality. Radio Practic 2023;38:210-5.

Cite this article as: Lei L, Zhou Y, Guo X, Wang L, Zhao X, Wang H, Ma J, Yue S. The value of a deep learning image reconstruction algorithm in whole-brain computed tomography perfusion in patients with acute ischemic stroke. Quant Imaging Med Surg 2023;13(12):8173-8189. doi: 10.21037/qims-23-547

